

**Universidade de Lisboa
Faculdade de Farmácia**



**Study of the cholestatic potential of relevant
concentrations of cyclosporine A in primary human
hepatocyte spheroids**

Tiago Miguel Gomes Antão

Mestrado Integrado em Ciências Farmacêuticas

2020

Universidade de Lisboa
Faculdade de Farmácia



**Study of the cholestatic potential of relevant
concentrations of cyclosporine A in primary human
hepatocyte spheroids**

Tiago Miguel Gomes Antão

Monografia de Mestrado Integrado em Ciências Farmacêuticas
apresentada à Universidade de Lisboa através da Faculdade de Farmácia

Orientador(a): Dr^a. Vânia Vilas-Boas e Prof. Mathieu Vinken

**Co-orientador(a): Professora Associada, Maria do Rosário de Brito
Correia Lobato**

2020



Erasmus+

This laboratory work was accomplished in the Department of *In Vitro* Toxicology of the Faculty of Medicine and Pharmacy at the Vrije Universiteit Brussel (VUB), under Erasmus+ Programme.

Brussels, Belgium



VRIJE
UNIVERSITEIT
BRUSSEL

Resumo

O fígado é o principal órgão responsável pelo metabolismo e excreção de compostos endógenos e exógenos, sendo o órgão mais exposto a compostos tóxicos. A colestase induzida por fármacos é causada pela acumulação tóxica de ácidos biliares nos hepatócitos, podendo a sua manifestação ter um início retardado. A colestase é uma patologia onde a secreção da bÍlis para o duodeno está reduzida, quer por reduzida funcionalidade dos hepatócitos, quer por obstrução da via secretória da bÍlis.

O principal objetivo desta investigação era o estudo dos efeitos da ciclosporina A a longo termo em culturas de esferóides de hepatócitos primários humanos.

Foi efetuado um estudo de dose-resposta durante 28 dias, onde as células eram expostas a diversas concentrações de fármaco. A viabilidade celular era medida pela quantificação do conteúdo total de ATP. Foi observado que a ciclosporina A era tóxica de forma dependente da concentração e tempo.

Para além disso, foi estudado os efeitos sinérgicos entre a ciclosporina A e os ácidos biliares. Os esferóides eram expostos a ciclosporina A na presença e na ausência de ácidos biliares durante 28 dias. Os resultados sugeriram que os esferóides ficavam sensibilizados pela ciclosporina A na presença de ácidos biliares, confirmando o seu sinergismo.

O índice colestático foi calculado para determinar que concentrações de ciclosporina A tinham o potencial de causar colestase. O índice colestático correspondia ao rácio entre o conteúdo de ATP dos hepatócitos na presença de ácidos biliares e o conteúdo de ATP dos hepatócitos na ausência de ácidos biliares. Valores inferiores ou iguais a 0.8 indicam que o composto tem o potencial de causar colestase. Os resultados demonstraram valores de índice colestático inferiores a 0.8, quando os esferóides estavam expostos a ciclosporina A a 5 µM, após 14 dias de exposição. De acordo com os resultados, a ciclosporina A foi considerada como exibindo potencial para induzir colestase.

Mais estudos podem ser realizados nesta área, de forma a descobrir por quais mecanismos a ciclosporina A induz colestase, dado que estes ainda não são totalmente compreendidos. Ensaio de RT-qPCR e Western Blot podem ser executados para estudar a expressão génica e proteica, respetivamente.

Palavras-chave: colestase; esferóides de hepatócitos primários humanos; ciclosporina A; efeitos sinérgicos dos ácidos biliares; índice colestático.

Abstract

The liver is the major organ responsible for the metabolism and excretion of endogenous and exogenous compounds, being more exposed to toxic compounds than any organ. Drug-induced cholestasis is attributed to the toxic accumulation of bile acids inside the hepatocytes and its manifestation can be delayed in onset. Cholestasis is a pathology where bile secretion to duodenum is reduced, whether by reduced functionality of the hepatocytes or obstruction of the excretory pathway of bile.

The main objective of this research was to study the long-term effects of cyclosporine A in primary human hepatocytes spheroid cultures.

A dose-response assay was conducted for 28 days, where the cells were exposed to several drug concentrations. Cell viability was measured by quantification of the total ATP content. It was assessed that cyclosporine A was toxic in a dose and time dependent manner.

Furthermore, it was studied the synergistic effects between cyclosporine A and bile acids. Spheroids were exposed to cyclosporine A in the presence and in the absence of bile acids for 28 days. Findings suggested that spheroids were sensitized to cyclosporine A in the presence of bile acids, therefore confirming their synergism.

Cholestatic index was calculated to determine which cyclosporine A concentrations had the potential to cause cholestasis. Cholestatic index was the ratio between the ATP content of the hepatocytes in the presence of bile acids and the ATP content of the hepatocytes in the absence of bile acids. Values lower than or equal to 0.8 indicated that the compound had the potential to cause cholestasis. Results showed cholestatic index values lower than 0.8, when spheroids were exposed to 5 μ M cyclosporine A after 14 days of drug exposure. According to the results, cyclosporine A was suggested to demonstrate potential to develop cholestasis.

More studies should be done in this area to discover by which mechanisms cyclosporine A induces cholestasis, since it is not yet fully understood. This can be achieved by performing RT-qPCR and Western Blot assays to study gene and protein expression, respectively.

Keywords: cholestasis; primary human hepatocyte spheroids; cyclosporine A; synergistic effects of bile acids; cholestatic index.

Index

1. Introduction	8
1.1. Cholestasis and drug-induced liver injury	8
Figure 1 – Simplified representation of the primary and secondary bile acids synthesis.	9
Figure 2 – Localization of bile acid transporters in human hepatocytes (1).	10
1.2. Primary human hepatocytes spheroids.....	10
1.3. Cyclosporine A.....	11
Figure 3 – Molecular structure of cyclosporine A (32).	11
2. Objectives	12
3. Materials and methods.....	12
3.1. Cell seeding.....	12
3.2. Assessment of lot viability	12
3.3. Dose-response assay	13
Figure 4 – Dose-response assay's representation.	13
3.4. Cholestatic index assay.....	14
Figure 5 – Dilution of each bile acids mix and DMSO in separate PHH media.....	14
3.5. ATP quantification viability assay.....	15
3.6. CDFDA and propidium iodide staining.....	16
4. Results	16
4.1. Assessment of lot viability	16
4.2. Formation of PHH spheroids.....	17
Figure 6 – Spheroid formation after seeding the cells in 96-well ultra-low attachment plates.	17
4.3. Cyclosporine A dose-response curve	17
Figure 7 – Cyclosporine A dose-response curve from day 1 to day 28 of the exposure with concentrations ranging from 0.01 μ M to 25 μ M.	18
4.4. Cyclosporine A and bile acids synergistic effect.....	18
Figure 8 – Synergistic effects of different concentrations of cyclosporine A with 30x concentrated bile acids mix.	18
4.5. Cholestatic index	19
Figure 9 – Cholestatic index of different concentrations of cyclosporine A from day 1 to day 28 of the exposure.....	19
4.6. Formation of bile canaliculi	19
Figure 10 – Images taken at day 5 of incubation of spheroids in different cyclosporine A concentrations with CDFDA and propidium iodide staining (arrows indicate functional bile canaliculi).....	20
5. Discussion.....	20
5.1. Assessment of lot viability	20

5.2.	Formation of PHH spheroids.....	21
5.3.	Cyclosporine A dose-response curve	21
5.4.	Cyclosporine A and bile acids synergistic effect.....	21
5.5.	Cholestatic index	22
5.6.	Formation of bile canaliculi	23
6.	Conclusion.....	24
7.	References.....	26
8.	Appendices.....	29
	Appendix A.....	30
	Appendix B.....	31
	Appendix C.....	32
	Appendix D.....	33
	Appendix E.....	34
	Appendix F.....	35
	Appendix G	36

1. Introduction

1.1. Cholestasis and drug-induced liver injury

The liver is a major vital organ that has a relevant role in our bodies. It is responsible for the metabolism and excretion of numerous endogenous and exogenous compounds. Since the liver is always accumulating several toxic compounds for detoxification, it is more predisposed to drug toxicity than any other organ (1,2). There are different types of injury that a drug can cause to the liver, depending on the mechanism that is causing it: hepatocellular, mixed or cholestatic (3). In this case, a drug related injury is classified as a drug-induced liver injury (DILI) (1).

DILI is one of the major concerns in drug development and chemical safety, with cholestasis accounting for almost 50% of all the DILI cases (4). DILI can lead to a wide variety of pathological conditions, but the predominant forms include acute hepatitis, cholestasis and a mixed pattern (5). The latter includes clinical manifestations of both hepatocellular and cholestatic injury (5). Despite rigorous testing practices, some severe adverse drug reactions are still only identified in the late stages of drug development and even post marketing, resulting in increased patient morbidity and expensive drug withdrawals (6). DILI is one of the primary causes for complications during clinical and preclinical studies and the main reason for drug withdrawal from the market (7,8). Therefore, DILI and cholestasis are important toxicity warnings to be taken into consideration in drug development (7). Current models to predict hepatotoxicity before a drug enters clinical stages include animal models and *in vitro* assays. However, the predictive power of animal models is limited due to relevant inter-species differences in the expression and activity of enzymes and transporters involved in drug absorption, distribution, metabolism and excretion (6,9). Consequently, the lack of ability of preclinical animal models to predict human potential for DILI is a substantial concern in the biotechnology and pharmaceutical industry (10). At last, in contrast to animal studies, *in vitro* experiments that use human cells represent models that offer the potential to investigate human-specific toxicity profiles (6,11,12).

Drug-induced cholestasis is associated with the toxic accumulation of bile acids in hepatocytes and considered to result from the modified functioning of the bile salt export pump (BSEP) caused by drugs, since this ATP-dependent transporter is the main responsible for the transport of bile acids, at the canalicular membrane (13,14). Moreover, the manifestation of this pathology is often complex and delayed in onset (14,15).

Cholestasis is characterized as a reduction in bile secretion and flow. There are many factors that can cause this pathology, such as reduced functionality of the hepatocytes in the secretion of bile and/or due to an obstruction of the excretory pathway of bile (16,17). Cholestasis can be caused by drugs, known as drug-induced cholestasis. Biochemical tests can be done to evaluate the liver function and to detect cholestasis. According to the Council of International Organizations of Medical Sciences (CIOMS), a cholestatic injury can be characterized by an elevation of serum alkaline phosphatase (AP) to greater than 2x the upper limit of normal (ULN) along with a major elevation of γ -glutamyl transpeptidase (GGT) in the presence of a normal alanine transaminase (ALT) value (1). Cholestasis may cause some unspecific symptoms such as nausea, anorexia and fatigue (18).

The pathogenesis of cholestasis can be better understood, once bile acids synthesis and bile formation and flow are explained. Cholesterol is used to synthesize primary bile acids, in the liver. Approximately 16 enzymes are involved in the synthesis of bile acids and the rate limiting step is the 7 α -hydroxylation by cytochrome P450 (CYP) isoform 7A1. In humans, the most common primary bile acids are chenodeoxycholic acid (CDCA) and cholic acid (CA)

(1,19). Primary bile acids can be converted to secondary bile acids by bacterial enzymes in the small and large intestine (19,20). The bile acids that enter the colon are metabolized by bacterial flora, where the primary bile acids, CDCA and CA, are converted into the secondary bile acids, lithocholic acid (LCA) and deoxycholic acid (DCA), respectively (Figure 1) (19). Under normal circumstances, bile acids are conjugated with glycine or taurine in hepatocytes, producing bile salts, to increase their hydrophilicity, facilitating their overall excretion (1,20). Bile acids enter hepatocytes, from the sinusoidal blood, mediated by the Na⁺-taurocholate cotransporting polypeptide (NTCP) and organic anion transporting polypeptides (OATPs) and are secreted into the bile flow principally by the bile salt export pump (BSEP) transport protein, at the canalicular membrane (Figure 2) (10,21). The multidrug resistance-associated protein 2 (MRP2) is responsible for the secretion of organic anions into the bile, mainly exporting reduced glutathione through the canalicular membrane, but also transports glucuronide and sulfate conjugates of bile acids (1,22).

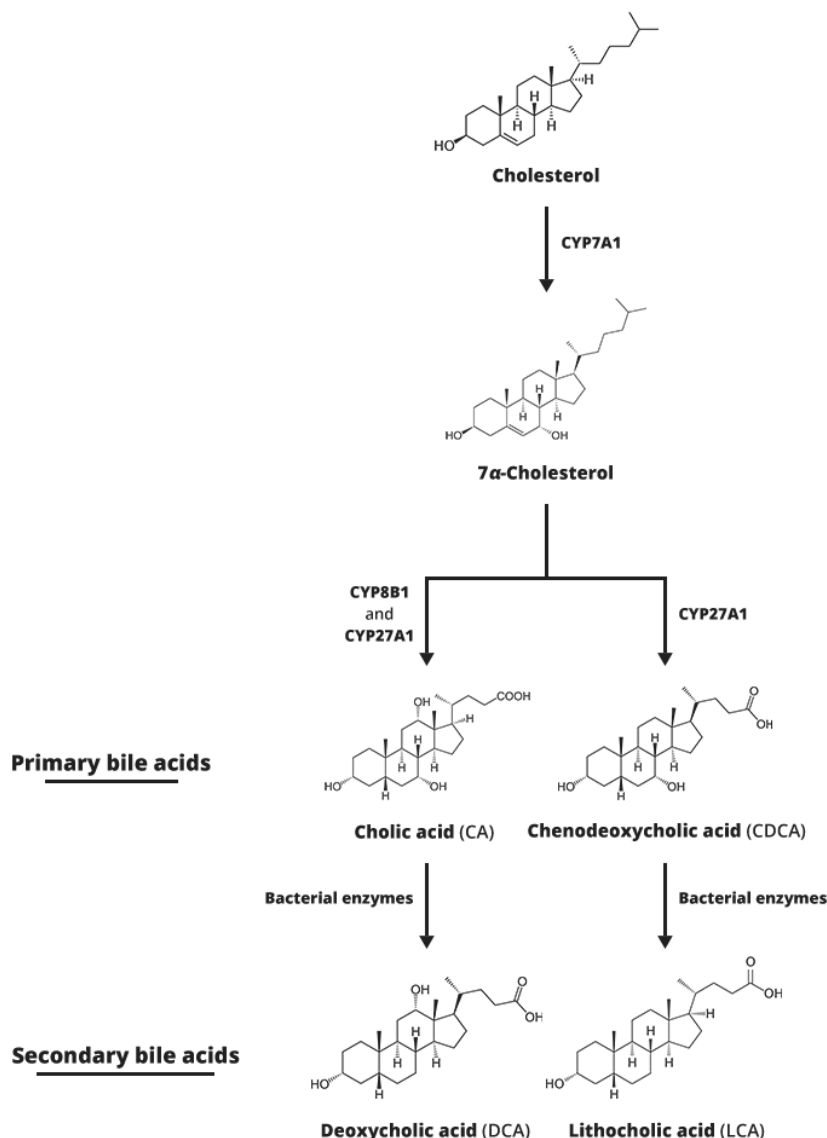


Figure 1 – Simplified representation of the primary and secondary bile acids synthesis.

After being released into the duodenum, bile acids have a relevant role in the digestion and absorption of dietary fat, fat-soluble vitamins and other lipophilic nutrients. Another important function of bile acids is that they facilitate the elimination of bile pigments, cholesterol

and other endogenous and exogenous metabolites (1,20). Bile acids can form mixed micelles with phospholipids and cholesterol in the bile, thus increasing cholesterol solubility and decreasing bile acids toxicity (20). This further promotes cholesterol elimination (1).

However, bile acids are toxic when accumulated in high concentrations in hepatocytes (23). It is believed that the toxicity is associated with hydrophobicity, being more toxic to the cell bile acids with higher hydrophobicity. In hepatocytes, bile acids are highly bound to cytosolic proteins. The concentration of unbound bile acids in the cell is usually low. Nevertheless, if bile acids accumulate in hepatocytes, cytosolic proteins would become saturated and would not bind to additional bile acid molecules. Therefore, the concentration of unbound bile acids would significantly increase, leading to mitochondrial damage and eventually to apoptosis or necrosis (1,23).

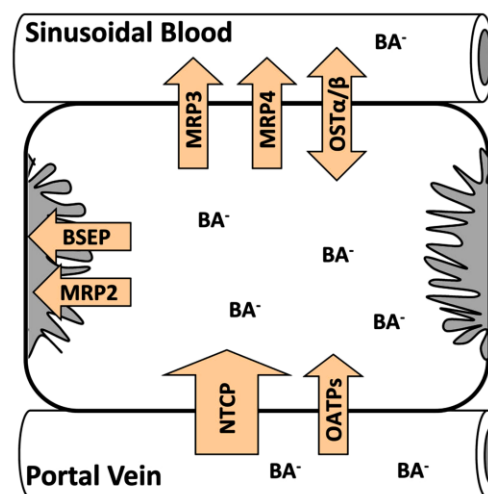


Figure 2 – Localization of bile acid transporters in human hepatocytes (1).

1.2. Primary human hepatocytes spheroids

A common strategy used to study different types of drug-induced liver injuries is by performing *in vitro* assays. Three-dimensional (3D) cell cultures have been used recently due to their similarity to *in vivo* systems and the advantages they have over two-dimensional (2D) cell cultures (24). Compared to *in vivo*, most of the cell-to-cell and cell-to-matrix interactions that are crucial for cell differentiation and proliferation, as well as cellular functions, are lost in 2D cell cultures. 3D models are more useful concerning their ability to mimic *in vivo* settings. Therefore, 3D cell cultures have been utilized for many applications such as differentiation, drug discovery, gene and protein expression, cellular physiology and pharmacological studies as well as cancer research and tissue engineering (24).

Some challenging obstacles arise when it comes to *in vitro* studies, including lack of cell systems to conduct long-term experiments, lack of scalability and cellular phenotype loss due to cell dedifferentiation, only allowing for short-term studies to be made (14,25). A cell model was required to study the potential effect of drugs to induce cholestasis in hepatocytes, in long-term studies. One approach to overcome these barriers involves the formation of 3D spheroids of primary human hepatocytes (PHH). This *in vitro* cellular system has been reported to mimic the *in vivo* human liver function (14,25,26). For the evaluation of DILI, PHH have been considered the gold standard model (6,27). There was an alternative cell model, the PHH sandwich culture, however, dedifferentiation started taking place after 2 weeks of culture, excluding its use for analysing the chronic toxicity of drugs (14). Overall, PHH spheroids provide a sensitive and robust system for long-term studies of drug-induced hepatotoxicity,

while the PHH sandwich culture has a more dedifferentiated phenotype and lower sensitivity to detect hepatotoxicity (6).

Spheroid cultures are stable and functional for up to 35 days, maintaining its metabolic activity over time and showing a proteome that resembles the liver *in vivo* (14,25). Hepatocytes' phenotype is less affected, as dedifferentiation occurs at a slower rate, which translates into stable liver-specific functionalities such as protein production and CYP activity. Additionally, cell-to-cell interactions are preserved and functional bile canaliculi are developed (14,25). Therefore, in order to study drug-induced cholestasis, PHH spheroids culture gathered all the requirements to perform a prolonged toxicity study.

1.3. Cyclosporine A

Cyclosporine A is a potent immunosuppressive agent and has been used against cellular rejection after solid organ transplantation (28,29). Cyclosporine A is a lipophilic cyclic polypeptide of 11 amino acids with a molecular weight of 1202 Daltons (Figure 3) (30). It is a secondary metabolite secreted by a fungal species, *Tolypocladium inflatum* (31,32). In plasma, only 10% is unbound and it binds to albumin and globulins, but predominantly to lipoproteins. The drug is mainly metabolized by CYP3A4 and CYP3A5, and approximately 95% of the metabolites are eliminated in the bile with only a small amount being excreted in the urine (29,30).

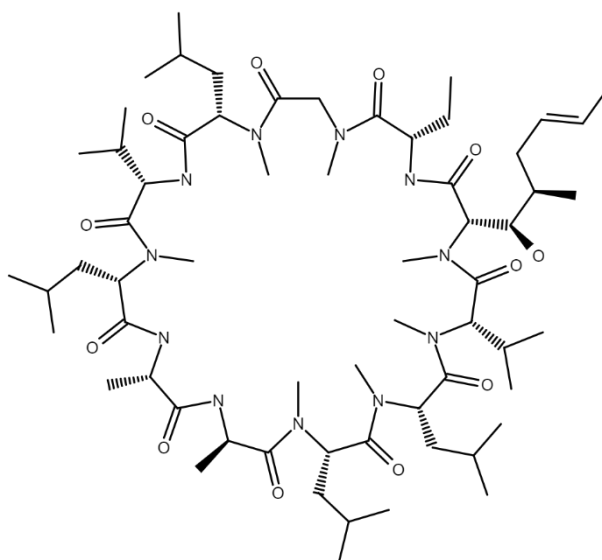


Figure 3 – Molecular structure of cyclosporine A (32).

As the major mechanism of action, cyclosporine A is a calcineurin inhibitor, leading to the suppression of the signal transduction pathway of T-cell activation (30,31). Calcineurin is a protein phosphatase that dephosphorylates regulatory sites on various transcription factors, when activated (30). In normal conditions, after calcineurin activation, the nuclear factor of activated T-lymphocytes (NFAT) is dephosphorylated by calcineurin, promoting cytokine genes transcription, including those of interleukin-2 (IL-2) and interleukin-4 (IL-4). However, when cyclosporine A enters T-cells, it binds to cyclophilins, leading to the blocking of calcineurin (30,31). Consequently, T-lymphocytes activation and cytokine genes transcription are inhibited, suppressing the overall immune response (30).

Studies show that cyclosporine A exhibits cholestatic effect in humans and in *in vitro* models (28). Cyclosporine A is a substrate for an organic cation transporter, P-glycoprotein

(P-gp) (33). There are still some gaps in the establishment of the cyclosporine A-induced cholestasis mechanisms, but some authors reported that cyclosporine A revealed a competitive inhibition of ATP-dependent transport of bile acids at the canalicular membrane, that could lead to an impairment of bile acids homeostasis (28,33,34). Furthermore, cyclosporine A is capable of inhibiting BSEP, MRP2 and NTCP's activity (34–36). Additionally, a reduction of the canalicular membrane fluidity was also another proposed explanation (28).

2. Objectives

The main objectives of this research were to study the long-term effects of cyclosporine A in primary human hepatocytes (PHH) spheroid cultures and to dig deeper into the mechanisms by which cyclosporine A induces cholestasis.

The methods planned to explore the mechanisms of cholestasis induced by cyclosporine A were the RT-qPCR and Western Blot techniques. However, these procedures could not be performed due to the SARS-CoV-2 pandemic.

3. Materials and methods

3.1. Cell seeding

The vial with the cryopreserved primary human hepatocytes (PHH) (purchased from KaLy-Cell) was thawed in Milli-Q (MQ) water at 37°C in the water bath. Once the contents were thawed, they were transferred to a falcon tube containing thawing medium (Universal Cryopreservation Recovery Medium) (IVAL), previously warmed at 37°C. Then, the falcon tube was gently mixed and centrifuged at 100g for 10 minutes, at room temperature. After the centrifugation, the supernatant was discarded and the pellet was resuspended with the remaining medium. Later, 4 mL of cold seeding medium (see Appendix A) were added to the falcon tube. Cell viability was, then, determined by counting the cells using Trypan Blue staining (see 3.2). After, the cell suspension was diluted to 30 000 cells/mL in seeding medium. In 96-well ultra-low attachment (ULA) plates (Corning), 50 µL per well (1 500 cells/well) were seeded, after homogenization of the cell suspension, using a multichannel pipette with wide aperture tips (Eppendorf). Then, 50 µL of seeding medium were added per well and the plates were centrifuged at 130g for 2 minutes, at room temperature. At last, the plates were incubated at 37°C with 5% CO₂ and humidified atmosphere. The first medium change occurred after 5 days of incubation: 50 µL of medium per well were removed and 50 µL of PHH medium (see Appendix A) per well were added.

3.2. Assessment of lot viability

Trypan Blue exclusion test was used to calculate each lot's cell viability. This test allows to confirm that the cell viability is not too low for a long-term experiment to take place. This assay is based on the principle that viable cells do not let the dye enter the cell because of their membrane's integrity and selective permeability, whereas nonviable cells lack the latter properties, so they let the dye in. For that reason, viable cells are unstained and nonviable cells are stained blue.

First, 1 part of cell suspension and 1 part of Trypan Blue (Bio-Rad) were pipetted into an Eppendorf tube and homogenized by gently pipetting up and down (37). Then, one drop of the mix was applied to a hemacytometer. The hemacytometer was placed on the stage of a binocular microscope and the cells were focused. Viable (unstained) and nonviable (stained) cells were counted separately using a manual cell counter. The percentage of viable cells was calculated with the following formula (37):

$$\text{Cell viability (\%)} = \frac{\text{total number of viable cells}}{\text{total number of cells}} \times 100\% \quad (1)$$

3.3. Dose-response assay

Stock solution of cyclosporine A (Calbiochem), 50 mM, was used to prepare 9 diluted solutions in dimethyl sulfoxide (DMSO) (Sigma): 0.01 mM; 0.05 mM; 0.1 mM; 0.5 mM; 1 mM; 2.5 mM; 5 mM; 10 mM and 25 mM (see Appendix B). These solutions were 1 000 times concentrated regarding the concentrations needed for the drug exposure. They were frozen, at -20°C, and thawed, at room temperature, when needed.

In order to prepare the final dilutions for the exposure, PHH medium, previously warmed at 37°C, was pipetted into a 96-well deep well plate and, then, cyclosporine A was diluted 1:1 000 in each well, from lowest to highest concentration (see Appendix C). The final cyclosporine A concentration, in each well, was, respectively: 0.01 µM; 0.05 µM; 0.1 µM; 0.5 µM; 1 µM; 2.5 µM; 5 µM; 10 µM and 25 µM. A control solution was also prepared with DMSO (1:1 000 dilution) instead of cyclosporine A. Each mix was homogenized by aspirating and dispensing 3 times, in each well, using a multichannel pipette (Viaflo).

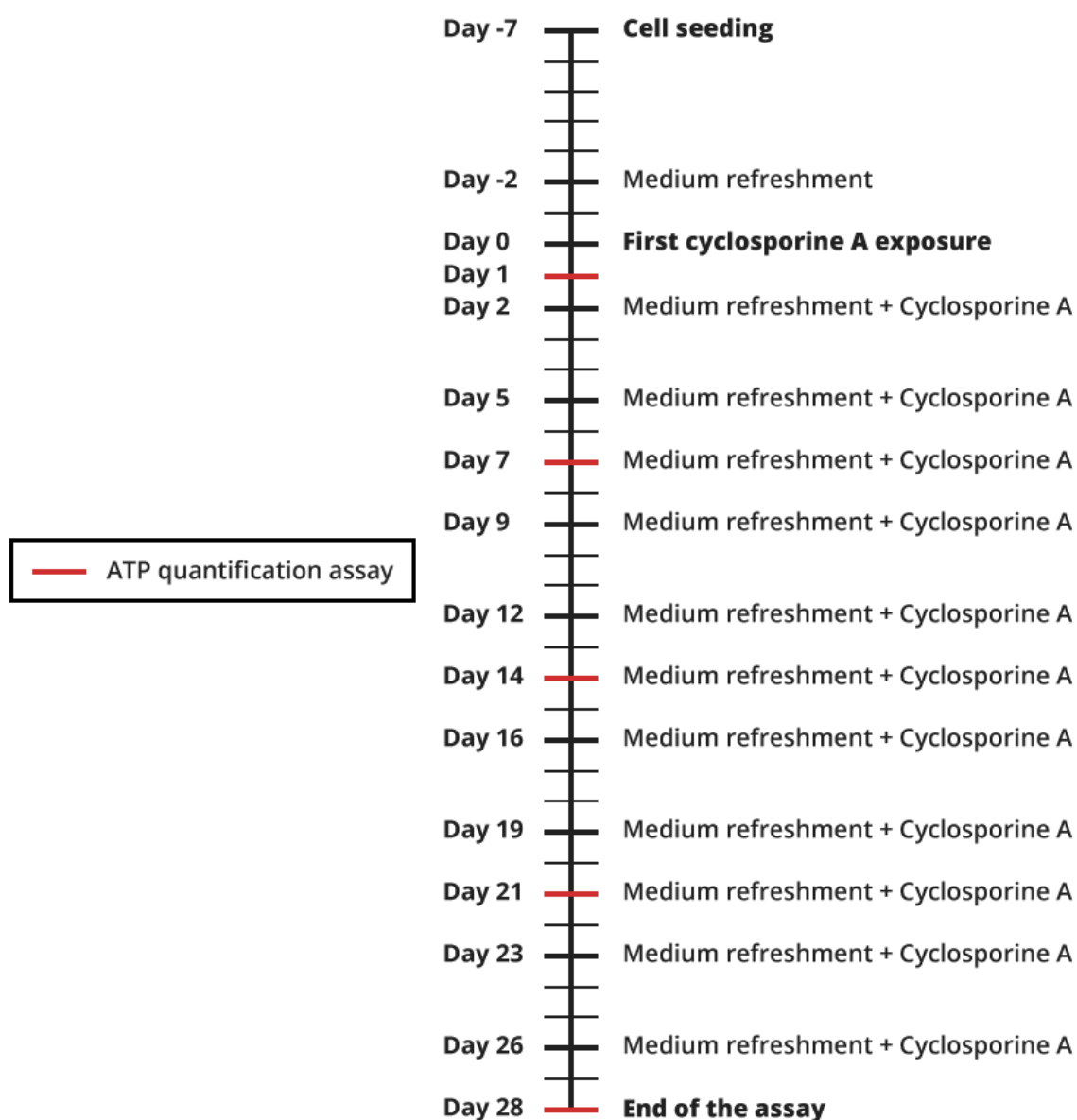


Figure 4 – Dose-response assay's representation.

The first cyclosporine A exposure was initiated 7 days after seeding the cells in the 96-well ULA plates. The exposures were made every 2 to 3 days and the first exposure counted

as day 0 (see Appendix D). At days 1, 7, 14, 21 and 28 of the exposure, the spheroids were collected to perform an ATP quantification assay (Figure 4). In the first exposure, 80 μ L of medium per well were removed and 90 μ L of 1:1 000 diluted cyclosporine A/control solution per well were added. In the following exposures, 80 μ L of medium per well were removed and 80 μ L of 1:1 000 diluted cyclosporine A/control solution per well were added. After the exposure, the plates were observed under the microscope to take note of the empty wells and, then, incubated at 37°C with 5% CO₂ and humidified atmosphere. The data obtained from this assay was converted into a chart using GraphPad software.

3.4. Cholestatic index assay

Stock solution of cyclosporine A, 50 mM, was used to prepare 4 diluted solutions in DMSO: 0.01 mM; 0.05 mM; 0.5 mM and 5 mM (see Appendix B). These solutions were 1 000 times concentrated regarding the concentrations needed for the drug exposure. They were frozen, at -20°C, and thawed, at room temperature, when needed for the exposure.

Five different bile acids were used in this assay: glycochenodeoxycholic acid (GCDCA), chenodeoxycholic acid (CDCA), glycodeoxycholic acid (GDCA), deoxycholic acid (DCA) and glycocholic acid (GCA). A mix of concentrated bile acids was prepared consisting of 79.2 mM of GCDCA; 23.4 mM of CDCA; 22.8 mM of GDCA; 24 mM of DCA and 21 mM of GCA (see Appendix E) (38). Since GCDCA and GDCA did not dissolve well in DMSO, one mix was made with Williams' Medium E, containing GCDCA and GDCA, and the other with DMSO, containing CDCA, DCA and GCA. These mixtures were 2 000 times concentrated than the concentration required in the well (a 30 times higher concentration of bile acids than physiological) (13,39–41). They were frozen, at -20°C, and thawed, at room temperature, when needed for the exposure.

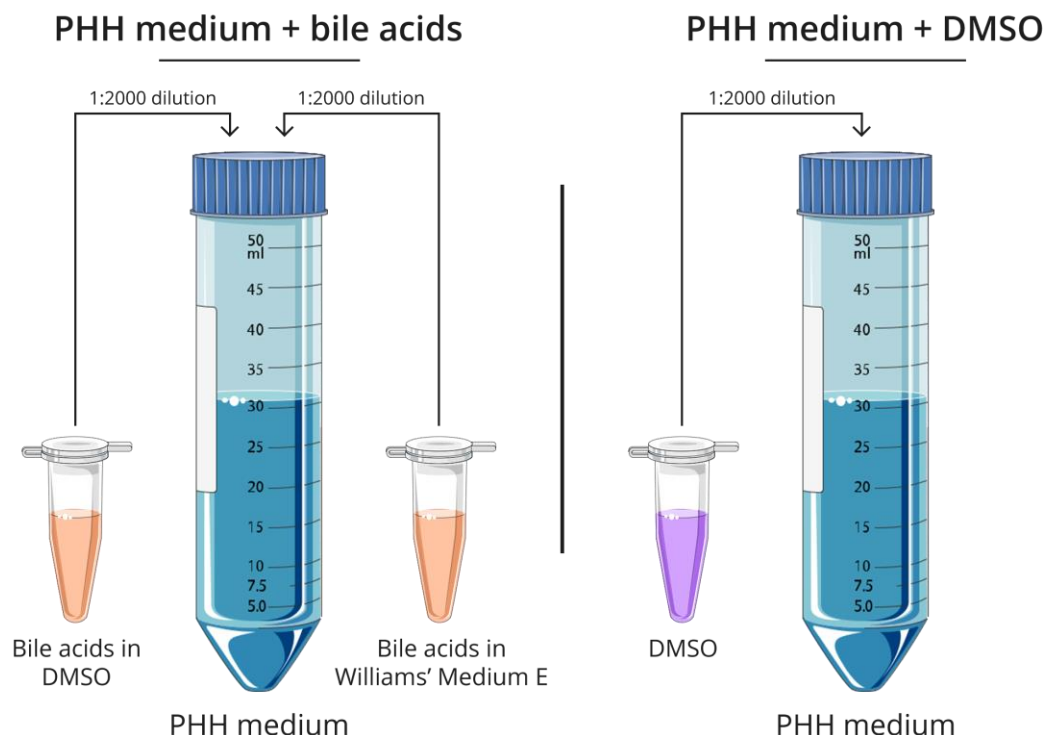


Figure 5 – Dilution of each bile acids mix and DMSO in separate PHH media.

Before the exposure, two separate PHH media, previously warmed at 37°C, were prepared, one with a 1:2 000 dilution of DMSO and the other with a 1:2 000 dilution of each bile acids mix (Figure 5). This resulted in a 30 times concentrated bile acids mix consisting of

39.6 μM of GCDCA; 11.7 μM of CDCA; 11.4 μM of GDCA; 12 μM of DCA and 10.5 μM of GCA (see Appendix E).

In order to prepare the final dilutions for the exposure, PHH medium with DMSO and PHH medium with the bile acids mix were pipetted separately into a 96-well deep well plate and, then, cyclosporine A was diluted 1:1 000 in each well, per condition, from lowest to highest concentration (see Appendix F). The final cyclosporine A concentration, in each well, was, respectively: 0.01 μM ; 0.05 μM ; 0.5 μM ; 5 μM . A control solution was also prepared, per condition, with DMSO (1:1 000 dilution) instead of cyclosporine A. The mix was homogenized by aspirating and dispensing 3 times, in each well, using a multichannel pipette (Vialflo).

The first cyclosporine A exposure, with and without bile acids, was initiated 7 days after seeding the cells in the 96-well ULA plates. The exposures were made every 2 to 3 days and the first exposure counted as day 0 (see Appendix D). At days 1, 7, 14, 21 and 28 of the exposure, the spheroids were collected to perform an ATP quantification assay (see 3.5). In the first exposure, 80 μL of medium per well were removed and 90 μL of cyclosporine A, cyclosporine A with bile acids or control solution per well were added. In the following exposures, 80 μL of medium per well were removed and 80 μL of freshly prepared cyclosporine A, cyclosporine A with bile acids or control solution per well were added. After the exposure, the plates were observed under the microscope to take note of the empty wells and, then, incubated at 37°C with 5% CO_2 and humidified atmosphere.

At last, to evaluate the effect of the bile acids mix simultaneously with cyclosporine A on the spheroids, a cholestatic index (Clx) was calculated using the following formula (38):

$$\text{Cholestatic Index (Clx)} = \frac{\text{ATP luminescence}_{\text{Cyclosporine A + Bile acids}}}{\text{ATP luminescence}_{\text{Cyclosporine A}}} \quad (2)$$

Cholestatic index was used to clarify the cholestatic potential of cyclosporine A (42). A cholestatic index value of less than or equal to 0.8 could be considered as an indication for enhanced risk for *in vitro* cholestasis. Cholestatic index values between 0.8 and 0.5 showed moderate *in vitro* cholestasis risk and cholestatic index values lower than or equal to 0.5 demonstrated high *in vitro* cholestasis risk. Values higher than 0.8 did not represent *in vitro* cholestasis risk (38,43).

In addition, a safety margin (SM) was calculated for cyclosporine A, based on the lowest *in vitro* concentration (μM) yielding a Clx lower than or equal to 0.8 and the C_{max} (μM , mean peak plasma concentration in human obtained from literature) (13,38). Cyclosporine A had a C_{max} of 0.77 μM (13,15). SM was determined as follows (13,38):

$$\text{Safety Margin (SM)} = \frac{\text{Lowest concentration } (\mu\text{M}) \text{ yielding a Clx} \leq 0.8}{C_{\text{max}} (\mu\text{M})} \quad (3)$$

This assay's charts were made for better visualization of the obtained results using GraphPad software.

3.5. ATP quantification viability assay

Total ATP content has been used as a marker of cell viability. After the death of a cell, it loses the ability to produce more ATP and endogenous ATPases consume the remaining ATP from the cell's cytoplasm (44). A reagent containing detergent, ATPase inhibitors, luciferin and luciferase was employed to perform this assay (CellTiter-Glo 3D, Promega). The detergent is used to lyse the cells and release ATP from the cells. The ATPase inhibitors are used to stabilise the released ATP. Then, a reaction between the substrate, luciferin, and the ATP is catalysed by a luciferase, generating light proportional to the amount of ATP in the sample,

that can be recorded by a luminescence plate reader (44). A simplified representation of the reaction can be exemplified as follows:



At days 1, 7, 14, 21 and 28 after the exposure, CellTiter-Glo 3D was thawed for at least 1 hour, in the dark. Then, 70 μL of medium per well were removed from the respective 96-well ULA plate and the plate was observed under the microscope to take note of the empty wells. After, in a dark room, 30 μL of reagent per well were added in the dark. Homogenization of the mixture was achieved by pipetting up and down 10 times per well, using a multichannel pipette, starting from the wells with highest to lowest drug concentration, since lowest to highest ATP concentration was expected in that order. The plate was incubated at 37°C for 20 minutes, in the dark. After 20 minutes, 50 μL of the mix per well were transferred to a white opaque 96-well plate and protected from light. At last, the white opaque plate was inserted in a luminescence plate reader (PerkinElmer®, 1420, Victor3, USA) to measure luminescence.

Raw luminescence data of ATP content collected from the luminescence plate reader was converted into percentage of the control spheroid and analysed. GraphPad software was used to make charts for better understanding and discussion of the obtained results.

3.6. CDFDA and propidium iodide staining

Carboxydichlorofluorescein diacetate (CDFDA) staining was used to analyse the formation of bile canaliculi in the spheroids. CDFDA passively diffuses into hepatocytes and is hydrolysed by intracellular esterases to carboxydichlorofluorescein (CDF), which is, then, effluxed into the bile canaliculi by MRP2 transporters (45,46). This staining is used to evaluate MRP2 transporters' activity by the CDF excretion in the bile canalicular networks (47). Furthermore, with this method it is possible to assess whether MRP2 is being inhibited or not.

Propidium iodide staining is based on the dye exclusion principle (48). Propidium iodide is a fluorescent agent that does not enter viable cells or cells with an intact membrane (48,49). For that reason, the dye diffuses into nonviable cells and binds to double-stranded DNA, increasing its fluorescence emission (48,49).

At day 5 after the exposure, one control spheroid and two spheroids exposed to 0.5 μM and 5 μM of cyclosporine A were transferred from the 96-well ULA plate to three separate Petri dishes and pre-incubated at 37°C with Hanks' balanced salt solution (HBSS) (Gibco) containing 10 mM hydroxyethyl piperazineethanesulfonic acid (HEPES) for 10 minutes (see Appendix G). After 10 minutes, CDFDA in HBSS containing 10 mM HEPES (HBSS-HEPES) was added to all Petri dishes and the dishes were incubated at 37°C for 15 minutes. Then, propidium iodide was added to all Petri dishes and the dishes were incubated at 37°C for 5 minutes, after which the dyes were removed and the spheroids were washed with HBSS-HEPES. Subsequently, several pictures of each Petri dish with different staining were taken using fluorescence microscopy.

4. Results

4.1. Assessment of lot viability

After performing the Trypan Blue staining, a total of 158 cells were counted, being 136 of them viable and 22 nonviable. Then, cell viability of the lot was assessed using the following formula:

$$\text{Cell viability (\%)} = \frac{136}{158} \times 100\% = 86.1\% \quad (4)$$

Note: there were a total of 3 seedings of cells – 1 seeding for the cyclosporine A dose-response curve assay and 2 seedings for the cyclosporine A and bile acids synergistic effect assay. This result was obtained from 1 of the 2 seedings of the latter experiment.

4.2. Formation of PHH spheroids

After seeding the cells in 96-well ULA plates, microscope images were taken to follow the spheroid's development. At first, the cluster of cells did not have any particular shape. However, cells started to gradually group together as time passed by. By the end of seven days, the spheroid was fully formed and had a 3D structure that resembled a sphere (Figure 6).

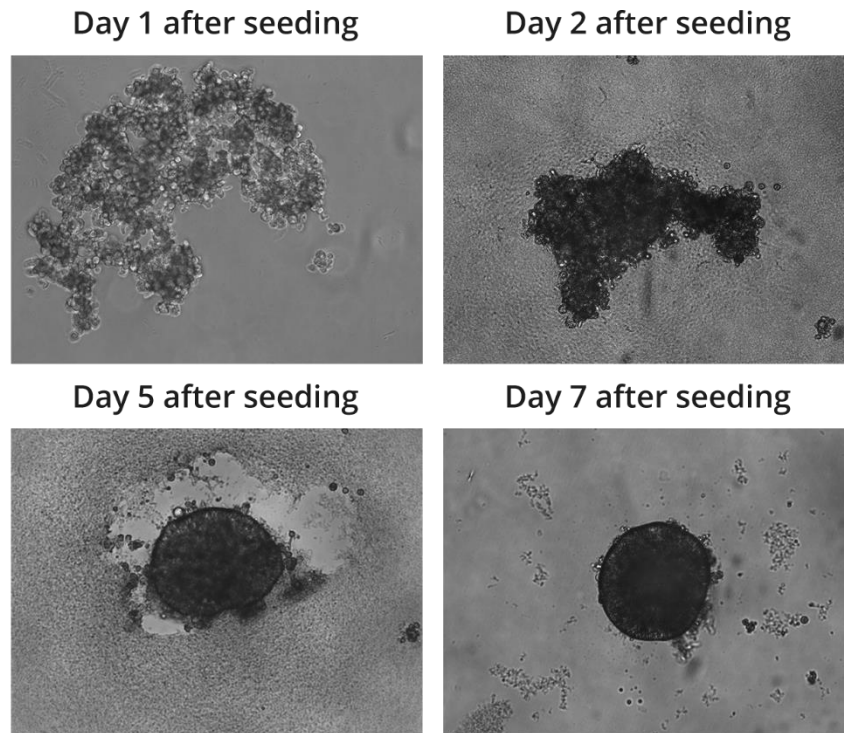


Figure 6 – Spheroid formation after seeding the cells in 96-well ultra-low attachment plates.

4.3. Cyclosporine A dose-response curve

The results from this experiment can be seen in Figure 7.

At day 1, ATP content did not differ much between different concentrations, except for the last two highest concentrations, 10 μM and 25 μM cyclosporine A, that had ATP content of approximately 80% of the control. At day 7, only the highest concentration had an ATP content below 50% of the control. At days 14, 21 and 28, the results were similar, showing that exposures of 10 μM and 25 μM cyclosporine A led to ATP content between 20% and 40%, and below 20% of the control, respectively.

As seen in the dose-response curve, cyclosporine A displayed time and concentration-dependent toxicity. Regarding the concentration-dependent toxicity, this translates into higher cell death when the spheroids are exposed to higher cyclosporine A concentrations. The time-dependent toxicity is demonstrated when the same concentration of drug leads to higher cell death after repeated and prolonged exposures.

The results from this assay helped to decide which cyclosporine A concentrations should be used on the cyclosporine A and bile acids synergistic effects assay. Highly toxic

concentrations could not be used, as the synergism with the bile acids would be difficult to be measured if most cells were killed by cyclosporine A alone.

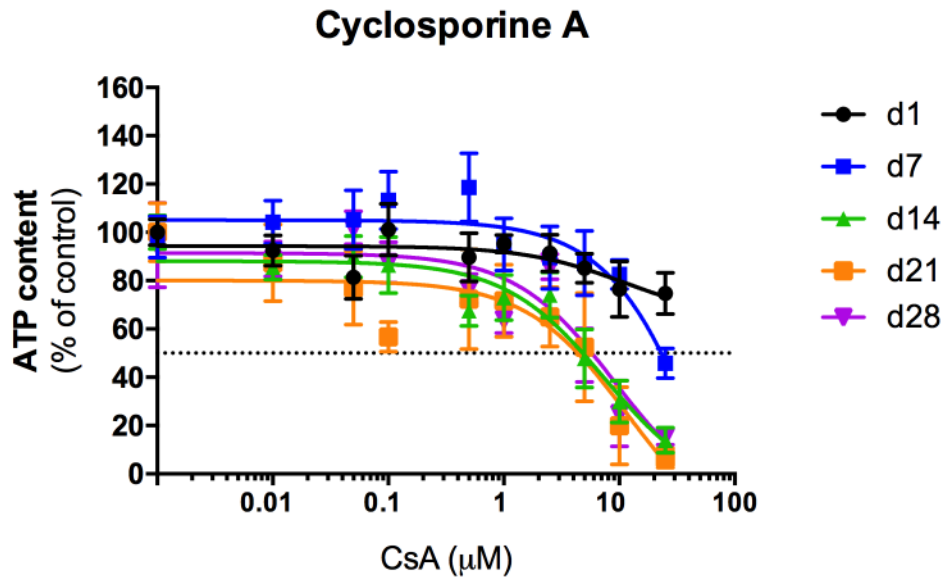


Figure 7 – Cyclosporine A dose-response curve from day 1 to day 28 of the exposure with concentrations ranging from 0.01 μM to 25 μM.

4.4. Cyclosporine A and bile acids synergistic effect

There was not a considerable variation of ATP content at 0.01 μM; 0.05 μM and 0.5 μM cyclosporine A concentrations without bile acids, on all endpoints. The most important variations in cell viability were noticed when PHH spheroids are exposed to cyclosporine A at 5 μM both in the presence and in the absence of concentrated bile acids mix. The results are illustrated in Figure 8.

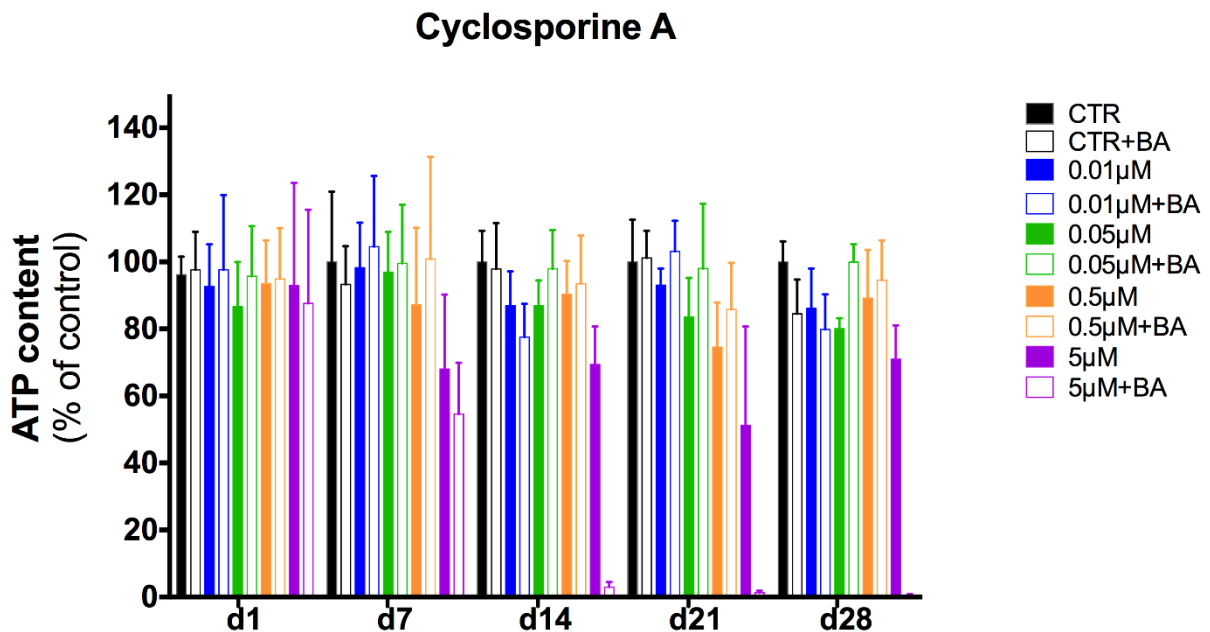


Figure 8 – Synergistic effects of different concentrations of cyclosporine A with 30x concentrated bile acids mix.

From day 1 to day 7, a considerable reduction of ATP content was observed at 5 μM cyclosporine A in the presence and absence of bile acids. Then, at day 14, the ATP content of

the condition with bile acids decreased to around 5% of the control and kept declining on the last two endpoints – days 21 and 28. However, the ATP content of 5 μM cyclosporine A alone did not vary much between days 7 and 28, remaining around and above 50%.

The results confirmed that cyclosporine A and bile acids displayed synergistic effects. After repeated exposures at the highest drug concentration, the presence of bile acids led to higher loss of cell viability when compared to the same condition without bile acids. In other words, bile acids sensitized the hepatocytes towards the cholestatic action of cyclosporine A.

4.5. Cholestatic index

These results were obtained from the results of the previous assay by applying the formula (2) to calculate the cholestatic index values. The results are shown in Figure 9.

Cholestatic indexes are above the 0.8 threshold throughout 28 days of exposure for all conditions, except for the highest concentration of cyclosporine A tested, 5 μM . The cholestatic index was below 0.8 at days 14, 21 and 28 for the highest cyclosporine A concentration, while it remained above the threshold at days 1 and 7. According to the results, cyclosporine A demonstrates *in vitro* cholestasis risk with a SM of 6.49. SM was calculated using formula (3), knowing that the lowest cyclosporine A concentration yielding a cholestatic index lower than or equal to 0.8 was 5 μM .

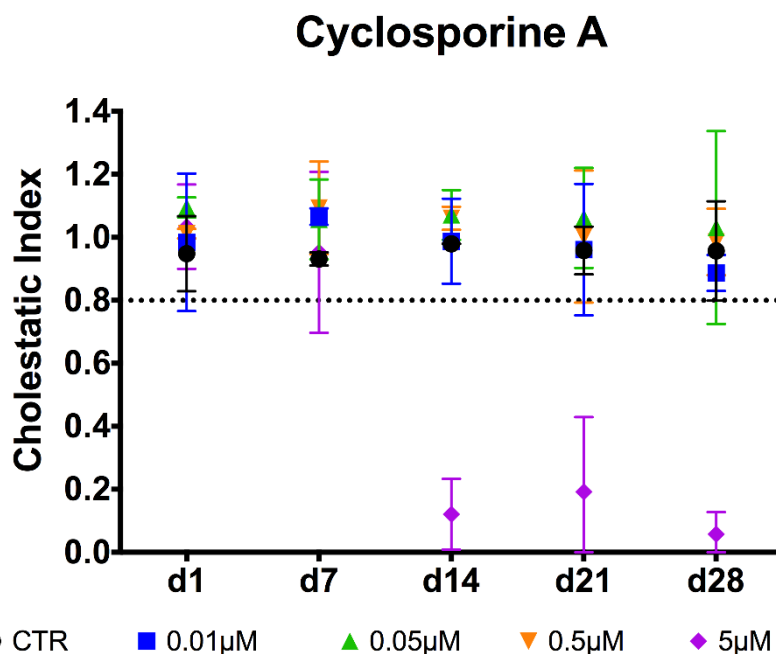


Figure 9 – Cholestatic index of different concentrations of cyclosporine A from day 1 to day 28 of the exposure.

4.6. Formation of bile canaliculi

Five days after the spheroids were first exposed to cyclosporine A, images were taken of a control spheroid and spheroids exposed to 0.5 μM and 5 μM cyclosporine A, respectively (Figure 10). CDFDA and propidium iodide staining were used to observe the activity of MRP2 transporters and cell death, respectively, in the spheroids.

Bile canaliculi can be seen in the control spheroid and in the 0.5 μM cyclosporine A-treated spheroid, whereas the spheroid exposed to 5 μM cyclosporine A did not have any visible. This finding suggested that MRP2 transporters' activity was inhibited when the spheroid was exposed to 5 μM cyclosporine A and MRP2 inhibition led to decreased transport of CDF into the bile canaliculi. Moreover, CDF was most likely trapped inside the hepatocytes, due to MRP2 inhibition, and the reduced fluorescence signal compared to the control condition could

be attributed to decreased cell viability, corroborated by the increased propidium iodide staining. CDFDA would only be converted to the fluorescent compound, CDF, if the cells were viable in the first place.

Compared to the control spheroid, the spheroid exposed to 5 μ M cyclosporine A showed more stained nuclei and a greater fluorescence emission, translating into greater cell death.

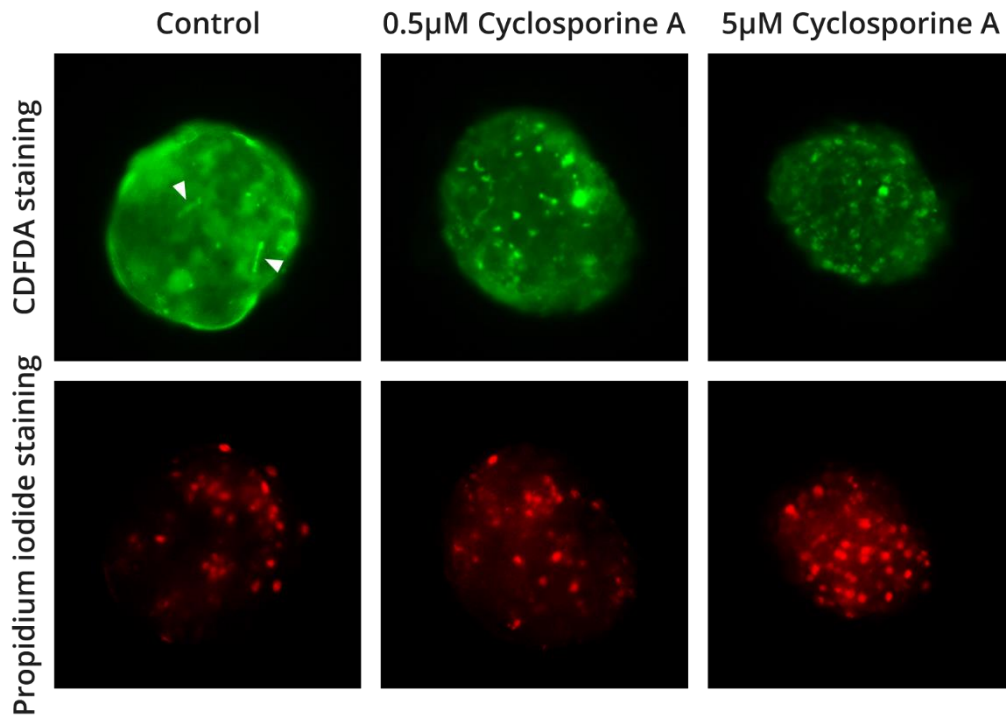


Figure 10 – Images taken at day 5 of incubation of spheroids in different cyclosporine A concentrations with CDFDA and propidium iodide staining (arrows indicate functional bile canaliculi).

5. Discussion

5.1. Assessment of lot viability

Assessment of lot viability is always done before seeding the cells, since it is a way to guarantee that the cells have the expected viability after thawing the vial containing the PHH. In case of lower viabilities than expected, hepatocytes would not probably be suitable for long experiments, because the number of cells from the starting point would already be low.

According to the lot's certificate of analysis, lot viability after thawing should be higher than 70%. A value of 86.1% for lot viability was calculated after performing the Trypan Blue staining assay and counting the viable and nonviable cells under the microscope, meaning that a high cell viability was obtained.

However, Trypan Blue staining despite being a quick and simple technique to execute, it has some limitations (37). The principle of this dye exclusion assay is based on the cell's integrity. Therefore, the viability of a cell can still be compromised, while retaining its membrane integrity. It is possible that a compromised cell develops repairing mechanisms to become fully viable again. Additionally, another problem arises from the subjective character of this assessment. A nonviable cell can be easily dismissed if a small amount of dye is in the cell. A

possible alternative would be the use of a fluorescent dye and fluorescence microscopy, as it gives more accurate results compared to Trypan Blue (37).

Furthermore, another alternative and a more advanced method of measuring cell viability is to determine the cell's light scatter characteristics by using flow cytometry with the help of propidium iodide. Nevertheless, this technique is more time consuming and is required only when precise measurements on the number of nonviable cells in a cell mixture must be obtained (37).

5.2. Formation of PHH spheroids

Several images were taken after the seeding to track the aggregation of the cells and, consequently, the formation of the spheroid. At first, 1 500 cells are dispersed in the well but, then, these start to aggregate, until a spheroid with a well-defined cell membrane is finally formed.

In line with a previous study, the spheroids took seven days to become fully developed (26). Once the spheroid culture is established, long-term experiments can take place to study drug-induced liver injuries, as it mimics human liver *in vivo* functions (26).

5.3. Cyclosporine A dose-response curve

This long-term assay consisted of treating spheroids with numerous concentrations of cyclosporine A for 28 days. Spheroids were exposed to nine different concentrations: 0.01 μM ; 0.05 μM ; 0.1 μM ; 0.5 μM ; 1 μM ; 2.5 μM ; 5 μM ; 10 μM and 25 μM . There was also a control condition in the absence of the compound.

Cell viability is measured by quantification of the total ATP content. High percentage of ATP content correlates with high cell viability.

As the results demonstrate, cyclosporine A's toxicity is dose and time dependent. Higher cyclosporine A concentrations led to higher toxicity in hepatocytes. Cyclosporine A at 10 μM and 25 μM showed considerable toxicity in the hepatocytes, as a relevant loss of cell viability was noted after the 14th day. In contrast, low concentrations of the drug, from 0.01 μM to 1 μM , suggested low toxicity in the spheroids, even in long-term exposures.

Overall, a similar pattern of results was obtained in previous studies. In one of them, HepaRG spheroids were treated with concentrations of cyclosporine A between 0.1 μM and 100 μM for 6 days and the drug showed a concentration-dependent toxicity – increased cell death was seen with higher compound concentrations (4). Additionally, other study demonstrated that PHH spheroids had lower viability when exposed to cyclosporine A for long periods of time (15). PHH spheroids were treated with the drug for 14 days at a concentration range of 0.7-20 μM . Time-dependent toxicity can be noticed, as the same compound concentration leads to higher cell death when the PHH spheroids are treated for a longer time. For example, nontoxic concentrations in short-term exposures may lead to cytotoxicity after repeated long-term exposures. Also, decreased cell viability was reported with higher cyclosporine A concentrations, revealing its dose-dependent toxicity (15). At last, it was observed, in another research, that cyclosporine A exhibited toxicity in some batches of sandwich-cultured rat hepatocytes (SCRH) when they were exposed for 24 hours at a concentration of 20 μM (47).

5.4. Cyclosporine A and bile acids synergistic effect

The main goal of this experiment was to assess if bile acids had synergistic effects with cyclosporine A in human hepatocytes, therefore supporting a cyclosporine A-associated cholestatic risk. PHH spheroids were exposed to cyclosporine A in the presence or absence

of a 30x concentrated bile acids mix for 28 days. Four different concentrations of the drug were employed: 0.01 μM ; 0.05 μM ; 0.5 μM and 5 μM .

The bile acids mixture utilized in this experiment is 30 times more concentrated than the physiological concentration of bile acids in the plasma, since their accumulation becomes relevant in case of cholestasis (38). Physiological hepatic concentrations of bile acids have been reported to reach 430-800 μM during cholestasis (38,50,51). The 30x concentrated bile acids mix was selected regarding that it would not, *per se*, significantly affect the viability of the culture. However, when the spheroids are co-exposed with the bile acids mix and increasing concentrations of a cholestatic compound, increased toxicity should be noted (38).

The previous experiment determined which cyclosporine A concentrations should be used on this assay. Concentrations that led to high loss of viability throughout the experiment could not be used, since it was expected that the presence of concentrated bile acids mix simultaneously with cyclosporine A would lead to lower cell viability compared to the exposure to cyclosporine A alone. If cell viability would be already low with the compound alone, the synergistic effects of bile acids could not be properly measured. Besides that, highly toxic cyclosporine A concentrations could not be utilized in an assay that lasted 28 days, as most of the cell viability would be lost by day 14 of the assay.

From the results, it is clear that cyclosporine A and bile acids display synergistic effects, in PHH spheroids, in a dose and time-dependent manner. For concentrations from 0.01 μM to 0.5 μM , no correlation could be seen that indicated the presence of synergistic effects. However, at 5 μM cyclosporine A, a small increase in toxicity could be observed on the condition with bile acids compared to the condition with the compound alone on day 7, that increased on the subsequent endpoints. By the end of the assay, a viability close to 0% of the control was obtained for cyclosporine A at 5 μM with bile acids, while in the absence of bile acids, cell viability remained around 70%. Although some loss of cell viability can be attributed to plate handling, the results appear to be in line with other findings (15).

In conclusion, these findings suggest that at the highest concentration of cyclosporine A and in the presence of bile acids, the hepatocytes showed decreased ability to dispose of the added bile acids, consistent with the inhibition of the BSEP transporter, resulting in the accumulation of intracellular bile acids up to toxic concentrations that lead to cell death. Moreover, according to previous studies that also used PHH spheroid cultures, increasing the time of exposure intensified the synergistic toxicity of cholestatic drugs and bile acids (14,15).

5.5. Cholestatic index

Data collected from the previous assay was used to calculate the cholestatic index at different drug concentrations, on every endpoint.

Cholestatic index is the ratio between the ATP content of the spheroids exposed to cyclosporine A in the presence of bile acids and the ATP content of the spheroids exposed to cyclosporine A in the absence of bile acids. A threshold of 0.8 was previously set to distinguish concentrations that can lead to cholestasis from concentrations that may have no potential to cause it. Cholestatic index values higher than 0.8 indicate mild or no potential to cause cholestasis, whereas values between 0.8 and 0.5 show moderate cholestasis risk (38). At last, a cholestatic index lower than or equal to 0.5 suggests high cholestasis risk (38).

Cholestatic index values lower than 1 imply that cell death is greater when hepatocytes are in the presence of bile acids. For example, a value of 0.8 means that the cell viability of the condition with the compound and bile acids is 80% of the condition with the compound alone.

According to the results, cyclosporine A is suggested to demonstrate high risk to cause cholestasis, with a SM of 6.49, when present for prolonged periods of time at a concentration of 5 μM . The first evidence of cholestatic risk appeared on the 14th day of the exposure with a cholestatic index lower than 0.2. By the end of the assay, a value of cholestatic index lower than 0.1 was obtained. Lower concentrations did not show any sign of cholestatic risk throughout the assay, as cholestatic index values were constantly above the threshold.

A similar result was achieved by a previous study. PHH spheroids were exposed to different concentrations of cyclosporine A, ranging from 0.7 μM to 20 μM , in the presence and absence of a 30x concentrated bile acids mix for 14 days (15). The bile acids mix was composed by the same 5 bile acids used in our assay. The exposure was initiated after spheroid formation and they were treated every second day with cyclosporine A with and without the bile acids mix. The obtained cholestatic index values were calculated with the highest concentration of the compound employed (20 μM). The synergistic toxicity of cyclosporine A and bile acids became more evident over time, since cholestatic index values of 0.66, 0.22 and 0.01 were attained after 3, 7 and 14 days of repeated exposure, respectively (15). This suggests that prolonged and repeated exposures to cyclosporine A increase its cholestatic properties in PHH spheroids (15). A short-term exposure of 3 days with 20 μM cyclosporine A indicated to be sufficient to display the synergistic effects of cyclosporine A and bile acids. Comparing with our findings, the first sign of synergism was only observed after 14 days of exposure to the drug. This could be explained by the fact that the highest concentration of cyclosporine A used in our assay was 4 times lower (5 μM) than in the previous study (20 μM). Also, a similar cholestatic index was acquired between 7 days of exposure with 20 μM cyclosporine A and 14 days of exposure with 5 μM cyclosporine A. This comparison indicates that with a lower and more clinically relevant concentration of cyclosporine A, a longer time of exposure is required to achieve an equivalent level of toxicity.

Furthermore, another study, using a different cell model, was conducted in order to assess the cholestatic potential of cyclosporine A. Several batches of freshly isolated rat hepatocytes in sandwich culture were incubated with different concentrations of cyclosporine A in the presence and absence of a 60x concentrated bile acids mix for a period of 24h (47). SCRH were exposed to 10 μM , 15 μM and 20 μM cyclosporine A. The toxicity of 10 μM cyclosporine A slightly increased in the presence of bile acids. However, when SCRH were exposed to 15 μM and 20 μM cyclosporine A, a significantly higher toxicity was noticed in the presence of the 60x concentrated bile acids mixture (47). A concentration-dependent decrease of cholestatic index values was observed in all batches. The mean cholestatic index values at 10 μM , 15 μM and 20 μM of cyclosporine A were found to be 0.89, 0.51 and 0.42, respectively (47). The compound can be considered as cholestatic, since both cholestatic indexes of the last 2 concentrations were lower than 0.8. Overall, a concentration-dependent increase in cholestatic potential was noted and an increased toxicity was detected when SCRH were co-exposed with cyclosporine A and the bile acids mix (47).

5.6. Formation of bile canaliculi

CDFDA and propidium iodide staining was used to evaluate MRP2 transporters' activity and cell death within the spheroid. Functional bile canaliculi can be seen in CDFDA staining via fluorescence microscopy, considering MRP2 is not being inhibited, since the hydrolysed product of CDFDA, CDF, can be transported from the hepatocytes into the bile canaliculi by MRP2 transporters (45). CDF is a specific substrate for MRP2 (36).

The results suggested that MRP2 transporters' activity was inhibited when hepatocytes were exposed to 5 μM cyclosporine A, as bile canaliculi were not seen compared to the control condition. Therefore, bile canaliculi could be found in the control and 0.5 μM cyclosporine A-treated conditions, where MRP2 inhibition did not take place. A previous report shown that

cyclosporine A at 10 μM and 50 μM concentrations have inhibited canalicular efflux of CDF in HepaRG cells after 2 hours of exposure (36).

Although it is not presented in this study's results, questions regarding the effects of cyclosporine A in the stability of bile canaliculi may arise. In the aforementioned study, control cells as well as cells exposed to 10 μM cyclosporine A did not show any changes in the bile canaliculi (36). However, when exposed to 50 μM cyclosporine A, bile canaliculi were constricted after 2 hours of exposure. Further bile canaliculi structure modifications, such as retraction and disappearance, were seen in 50 μM cyclosporine A-treated cells (36).

6. Conclusion

The liver is constantly exposed to harmful compounds due to its main detoxifying function. Regarding its nature, the liver is more susceptible to injury than any other organ. When it develops a pathology due to the constant use of drugs, it can be classified as a DILI. Depending on the mechanism that is causing the injury, DILIs can be divided into 3 types: hepatocellular, mixed and cholestatic.

Regarding the relevant impact of DILI on public health and drug development, it is crucial to better understand the underlying mechanisms that lead to injury, with the aim of preventing this major issue. Although thorough studies are conducted by the pharmaceutical industry to assure the safety of a drug, some adverse drug reactions may be found after the drug has been released to the market, potentially leading to its withdrawal from the marketplace. The delayed onset of drug-induced cholestasis is one of the main reasons for the market withdrawal of the drug, since it is difficult to be observed during preclinical studies.

PHH spheroids are of great importance to study DILI due to their suitability for long-term experiments to study prolonged effects of xenobiotics *in vitro*. This cellular model is stable for up to 35 days. In addition, spheroids take 7 days to be fully formed after seeding and, then, they can be employed in experiments for 28 days. 3D PHH cultures may help reduce the quantity of animal models used in toxicity studies, while obtaining reliable results, since PHH spheroids resemble the human liver *in vivo* in terms of function.

Cyclosporine A is toxic in a time and concentration-dependent manner. A nontoxic drug concentration can become toxic after repeated exposures in an extended period of time. Furthermore, hepatocytes are more susceptible and sensitive to cyclosporine A at higher concentrations.

Moreover, cyclosporine A and bile acids displayed synergistic effects. In the presence of bile acids, hepatocytes exhibited increased sensitivity to cyclosporine A. Bile acids enhanced cyclosporine A's cytotoxicity. In a situation of cholestasis, bile acids' homeostasis is already disturbed due to reduced bile flow and secretion, meaning that bile acids are accumulating in hepatocytes. Cyclosporine A inhibits BSEP activity, therefore hepatocytes cannot eliminate the excess of bile acids inside the cell, since this transporter is the main responsible for the transport of bile acids.

Furthermore, cholestatic index values for cyclosporine A were below 0.8 after a long-term treatment and the margin of safety was 6.49. This indicates *in vitro* risk to induce cholestasis.

On a last note, further studies should be done to better understand cyclosporine A's mechanism to induce cholestasis. Although it is known that cyclosporine A is a BSEP inhibitor, more information could be obtained by performing assays to evaluate gene and protein

expression. Laboratory techniques, such as, RT-qPCR and Western Blot, should be performed, respectively, to study gene and protein expression.

7. References

1. Yang K, Köck K, Sedykh A, Tropsha A, Brouwer KLR. An updated review on drug-induced cholestasis: Mechanisms and investigation of physicochemical properties and pharmacokinetic parameters. *Journal of Pharmaceutical Sciences*. 2013 Sep;102(9):3037–57.
2. Padda MS, Sanchez M, Akhtar AJ, Boyer JL. Drug-induced cholestasis. *Hepatology*. 2011 Apr;53(4):1377–87.
3. Fontana RJ. Pathogenesis of idiosyncratic drug-induced liver injury and clinical perspectives. *Gastroenterology*. 2014 Apr;146(4):914-928.e1.
4. Ramaiahgari SC, Ferguson SS. Organotypic 3D HepaRG liver model for assessment of drug-induced cholestasis. In 2019. p. 313–23.
5. Stephens C, Andrade RJ, Lucena MI. Mechanisms of drug-induced liver injury. *Current Opinion in Allergy and Clinical Immunology*. 2014 Aug;14(4):286–92.
6. Bell CC, Dankers ACA, Lauschke VM, Sison-Young R, Jenkins R, Rowe C, et al. Comparison of hepatic 2D sandwich cultures and 3D spheroids for long-term toxicity applications: A multicenter study. *Toxicological Sciences*. 2018 Apr 1;162(2):655–66.
7. Kotsampasakou E, Ecker GF. Predicting drug-induced cholestasis with the help of hepatic transporters—An in silico modeling approach. *Journal of Chemical Information and Modeling*. 2017 Mar 27;57(3):608–15.
8. Watkins PB. Idiosyncratic liver injury: Challenges and approaches. *Toxicologic Pathology*. 2005 Jan 25;33(1):1–5.
9. Martignoni M, Groothuis GMM, de Kanter R. Species differences between mouse, rat, dog, monkey and human CYP-mediated drug metabolism, inhibition and induction. *Expert Opinion on Drug Metabolism & Toxicology*. 2006 Dec 24;2(6):875–94.
10. Cheng Y, Woolf TF, Gan J, He K. In vitro model systems to investigate bile salt export pump (BSEP) activity and drug interactions: A review. *Chemico-Biological Interactions*. 2016 Aug;255:23–30.
11. Soldatow VY, LeCluyse EL, Griffith LG, Rusyn I. In vitro models for liver toxicity testing. *Toxicol Res*. 2013;2(1):23–39.
12. Ewart L, Dehne E-M, Fabre K, Gibbs S, Hickman J, Hornberg E, et al. Application of microphysiological systems to enhance safety assessment in drug discovery. *Annual Review of Pharmacology and Toxicology*. 2018 Jan 6;58(1):65–82.
13. Oorts M, Baze A, Bachellier P, Heyd B, Zacharias T, Annaert P, et al. Drug-induced cholestasis risk assessment in sandwich-cultured human hepatocytes. *Toxicology in Vitro*. 2016 Aug;34:179–86.
14. Hendriks DFG, Fredriksson Puigvert L, Messner S, Mortiz W, Ingelman-Sundberg M. Hepatic 3D spheroid models for the detection and study of compounds with cholestatic liability. *Scientific Reports*. 2016 Dec 19;6(1):35434.
15. Parmentier C, Hendriks DFG, Heyd B, Bachellier P, Ingelman-Sundberg M, Richert L. Inter-individual differences in the susceptibility of primary human hepatocytes towards drug-induced cholestasis are compound and time dependent. *Toxicology Letters*. 2018 Oct;295(March):187–94.
16. Shah R, John S. Cholestatic jaundice. *StatPearls*. 2020.

17. Zollner G, Trauner M. Mechanisms of cholestasis. *Clinics in Liver Disease*. 2008 Feb;12(1):1–26.
18. Bhamidimarri KR, Schiff E. Drug-induced cholestasis. *Clinics in Liver Disease*. 2013 Nov;17(4):519–31.
19. Ajouz H, Mukherji D, Shamseddine A. Secondary bile acids: an underrecognized cause of colon cancer. *World Journal of Surgical Oncology*. 2014;12(1):164.
20. Li T, Apte U. Bile acid metabolism and signaling in cholestasis, inflammation, and cancer. In: *Physiology & Behavior*. 2015. p. 263–302.
21. Boyer JL. Bile formation and secretion. In: *Comprehensive Physiology*. Hoboken, NJ, USA: John Wiley & Sons, Inc.; 2013. p. 1035–78.
22. Dean M, Hamon Y, Chimini G. The human ATP-binding cassette (ABC) transporter superfamily. *Journal of Lipid Research*. 2001;42(7):1007–17.
23. Oizumi K, Sekine S, Fukagai M, Susukida T, Ito K. Identification of bile acids responsible for inhibiting the bile salt export pump, leading to bile acid accumulation and cell toxicity in rat hepatocytes. *Journal of Pharmaceutical Sciences*. 2017 Sep;106(9):2412–9.
24. Ravi M, Paramesh V, Kaviya SR, Anuradha E, Solomon FDP. 3D cell culture systems: Advantages and applications. *Journal of Cellular Physiology*. 2015 Jan;230(1):16–26.
25. Kozyra M, Johansson I, Nordling Å, Ullah S, Lauschke VM, Ingelman-Sundberg M. Human hepatic 3D spheroids as a model for steatosis and insulin resistance. *Scientific Reports*. 2018 Dec 24;8(1):14297.
26. Bell CC, Hendriks DFG, Moro SML, Ellis E, Walsh J, Renblom A, et al. Characterization of primary human hepatocyte spheroids as a model system for drug-induced liver injury, liver function and disease. *Scientific Reports*. 2016 Jul 4;6(1):25187.
27. Gómez-Lechón MJ, Tolosa L, Conde I, Donato MT. Competency of different cell models to predict human hepatotoxic drugs. *Expert Opinion on Drug Metabolism & Toxicology*. 2014 Nov 9;10(11):1553–68.
28. TAZUMA S. Cyclosporin A and cholestasis: Its mechanism(s) and clinical relevancy. *Hepatology Research*. 2006 Mar;34(3):135–6.
29. Parmentier C, Couttet P, Wolf A, Zaccharias T, Heyd B, Bachellier P, et al. Evaluation of transcriptomic signature as a valuable tool to study drug-induced cholestasis in primary human hepatocytes. *Archives of Toxicology*. 2017 Aug 10;91(8):2879–93.
30. Tedesco D, Haragsim L. Cyclosporine: A review. *Journal of Transplantation*. 2012;2012:1–7.
31. Matsuda S, Koyasu S. Mechanisms of action of cyclosporine. *Immunopharmacology*. 2000 May 27;47(2–3):119–25.
32. Patel D, Wairkar S. Recent advances in cyclosporine drug delivery: challenges and opportunities. *Drug Delivery and Translational Research*. 2019 Dec 29;9(6):1067–81.
33. Morisawa Y, Takikawa H. Effect of bile acids on the biliary excretion of pravastatin in rats. *Hepatology Research*. 2009 Jun;39(6):595–600.
34. Watkins PB, Seeff LB. Drug-induced liver injury: Summary of a single topic clinical research conference. *Hepatology*. 2006 Mar;43(3):618–31.

35. Kis E, Ioja E, Rajnai Z, Jani M, Méhn D, Herédi-Szabó K, et al. BSEP inhibition – In vitro screens to assess cholestatic potential of drugs. *Toxicology in Vitro*. 2012 Dec;26(8):1294–9.
36. Sharanek A, Azzi PB-E, Al-Attrache H, Savary CC, Humbert L, Rainteau D, et al. Different dose-dependent mechanisms are involved in early cyclosporine A-induced cholestatic effects in HepaRG cells. *Toxicological Sciences*. 2014 Sep 1;141(1):244–53.
37. Strober W. Trypan blue exclusion test of cell viability. In: *Current Protocols in Immunology*. Hoboken, NJ, USA: John Wiley & Sons, Inc.; 2001. p. 2–3.
38. Chatterjee S, Richert L, Augustijns P, Annaert P. Hepatocyte-based in vitro model for assessment of drug-induced cholestasis. *Toxicology and Applied Pharmacology*. 2014 Jan;274(1):124–36.
39. Scherer M, Gnewuch C, Schmitz G, Liebisch G. Rapid quantification of bile acids and their conjugates in serum by liquid chromatography–tandem mass spectrometry. *Journal of Chromatography B*. 2009 Nov;877(30):3920–5.
40. Xiang X, Han Y, Neuvonen M, Laitila J, Neuvonen PJ, Niemi M. High performance liquid chromatography–tandem mass spectrometry for the determination of bile acid concentrations in human plasma. *Journal of Chromatography B*. 2010 Jan;878(1):51–60.
41. Gnewuch C, Liebisch G, Langmann T, Dieplinger B, Mueller T, Haltmayer M, et al. Serum bile acid profiling reflects enterohepatic detoxification state and intestinal barrier function in inflammatory bowel disease. *World Journal of Gastroenterology*. 2009;15(25):3134.
42. Petrov PD, Fernández-Murga ML, López-Riera M, Gómez-Lechón MJ, Castell J v., Jover R. Predicting drug-induced cholestasis: Preclinical models. *Expert Opinion on Drug Metabolism & Toxicology*. 2018 Jul 3;14(7):721–38.
43. Deferm N, Richert L, van Brantegem P, de Vocht T, Qi B, de Witte P, et al. Detection of drug-induced cholestasis potential in sandwich-cultured human hepatocytes. In 2019. p. 335–50.
44. Riss TL, Moravec RA, Niles AL, Duellman S, Benink HA, Worzella TJ, et al. Cell viability assays. *Assay Guidance Manual*. 2004. 1–25.
45. Zamek-gliszczynski MJ, Xiong HAO, Patel NJ, Turncliff RZ, Pollack GM, Brouwer KIMLR. Dichlorofluorescein and its diacetate promoiety in the liver. *Pharmacology*. 2003;304(2):801–9.
46. Bachour-El Azzi P, Sharanek A, Burban A, Li R, Guével R le, Abdel-Razzak Z, et al. Comparative localization and functional activity of the main hepatobiliary transporters in HepaRG cells and primary human hepatocytes. *Toxicological Sciences*. 2015 May;145(1):157–68.
47. Oorts M, Richert L, Annaert P. Drug-induced cholestasis detection in cryopreserved rat hepatocytes in sandwich culture. *Journal of Pharmacological and Toxicological Methods*. 2015 May;73:63–71.
48. CHACON E, ACOSTA D, LEMASTERS J. Primary cultures of cardiac myocytes as in vitro models for pharmacological and toxicological assessments. In: *In Vitro Methods in Pharmaceutical Research*. Elsevier; 1996. p. 209–23.

49. Kainz K, Tadic J, Zimmermann A, Pendl T, Carmona-Gutierrez D, Ruckenstuhl C, et al. Methods to assess autophagy and chronological aging in yeast. In: *Methods in Enzymology*. 1st ed. Elsevier Inc.; 2017. p. 367–94.
50. Fischer S, Beuers U, Spengler U, Zwiebel FM, Koebe H-G. Hepatic levels of bile acids in end-stage chronic cholestatic liver disease. *Clinica Chimica Acta*. 1996 Jul;251(2):173–86.
51. Rolo AP, Palmeira CM, Wallace KB. Mitochondrially mediated synergistic cell killing by bile acids. *Biochimica et Biophysica Acta (BBA) - Molecular Basis of Disease*. 2003 Jan;1637(1):127–32.
52. Hanks JH, Wallace RE. Relation of oxygen and temperature in the preservation of tissues by refrigeration. *Experimental Biology and Medicine*. 1949 Jun 1;71(2):196–200.

Appendix A

Seeding medium and Primary Human Hepatocytes (PHH) medium composition

Seeding medium composition:

- Williams' Medium E (Gibco) – 500 mL
- L-glutamine-Penicillin-Streptomycin (Sigma-Aldrich) – 5.1 mL (0.91%)
- Insulin-Transferrin-Selenium (Gibco) – 5.1 mL (0.91%)
- Dexamethasone (1 mM in DMSO) – 51 μ L (0.01%)
- Fetal bovine serum (Gibco) – 50 mL (8.93%)

PHH medium composition:

- Williams' Medium E (Gibco) – 500 mL
- L-glutamine-Penicillin-Streptomycin (Sigma-Aldrich) – 5.1 mL (1.00%)
- Insulin-Transferrin-Selenium (Gibco) – 5.1 mL (1.00%)
- Dexamethasone (1 mM in DMSO) – 51 μ L (0.01%)

Appendix B

Cyclosporine A dilutions from stock solution

Table 1 – Cyclosporine A dilutions from stock solution.

[1 000x concentrated cyclosporine A solutions] (mM)	Final volume (µL)	Cyclosporine A (µL)	DMSO (µL)
25	50	25 µL from 50 mM stock	25
10	50	10 µL from 50 mM stock	40
5	50	5 µL from 50 mM stock	45
2.5	50	2.5 µL from 50 mM stock	47.5
1	50	1 µL from 50 mM stock	49
0.5	50	5 µL from 5 mM dilution	45
0.1	50	1 µL from 5 mM dilution	49
0.05	50	5 µL from 0.5 mM dilution	45
0.01	50	1 µL from 0.5 mM dilution	49

Appendix C

Dose-response assay plates layout

96-well deep well plate layout:

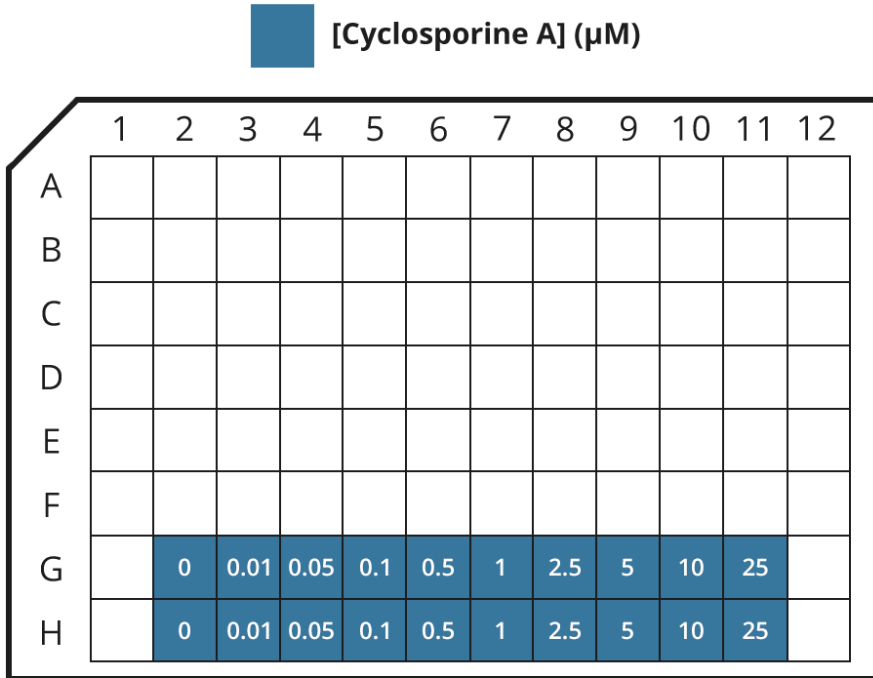


Figure 11 – 96-well deep well plate layout of cyclosporine A dilutions.

96-well ultra-low attachment plate layout:

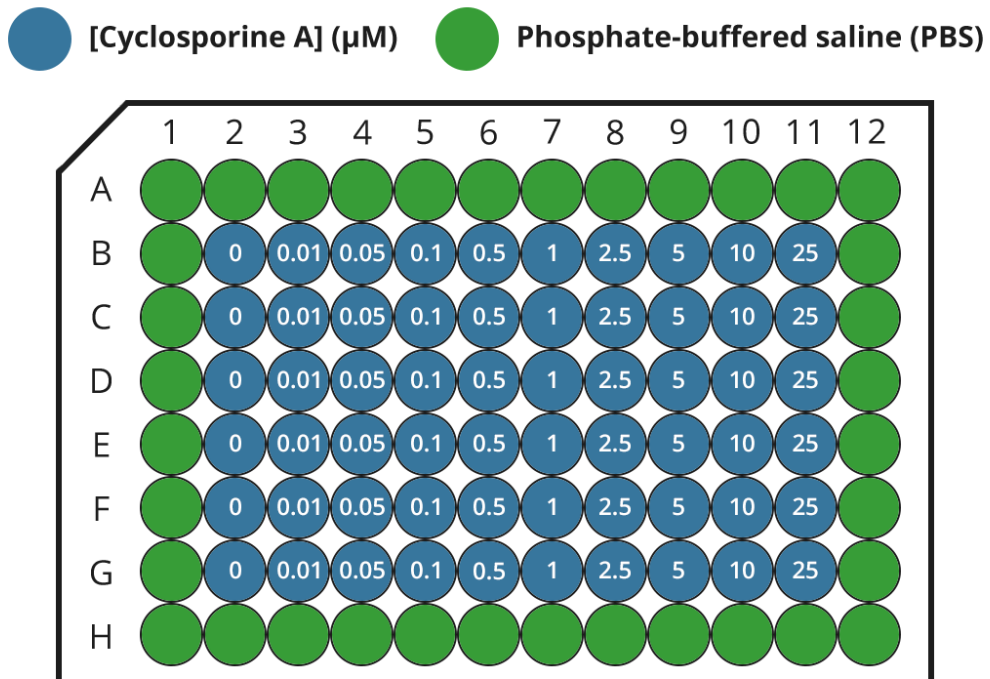


Figure 12 – 96-well ultra-low attachment plate layout of cyclosporine A exposure.

Appendix D

Dose-response and Cholestatic Index assays' schedule

Assays' schedule:

1. **Day -7: Cell seeding.**
2. Day -2:
 - a. Medium refreshment of five 96-well ULA plates.
3. **Day 0: First cyclosporine A exposure.**
 - a. Cyclosporine A exposure of five 96-well ULA plates.
4. **Day 1:**
 - a. ATP quantification assay of one 96-well ULA plate.
5. Day 2:
 - a. Medium refreshment of four 96-well ULA plates.
6. Day 5:
 - a. Medium refreshment of four 96-well ULA plates.
7. **Day 7:**
 - a. Medium refreshment of three 96-well ULA plates.
 - b. ATP quantification assay of one 96-well ULA plate.
8. Day 9:
 - a. Medium refreshment of three 96-well ULA plates.
9. Day 12:
 - a. Medium refreshment of three 96-well ULA plates.
10. **Day 14:**
 - a. Medium refreshment of two 96-well ULA plates.
 - b. ATP quantification assay of one 96-well ULA plate.
11. Day 16:
 - a. Medium refreshment of two 96-well ULA plates.
12. Day 19:
 - a. Medium refreshment of two 96-well ULA plates.
13. **Day 21:**
 - a. Medium refreshment of one 96-well ULA plate.
 - b. ATP quantification assay of one 96-well ULA plate.
14. Day 23:
 - a. Medium refreshment of one 96-well ULA plate.
15. Day 26: Last cyclosporine A exposure.
 - a. Medium refreshment of one 96-well ULA plate.
16. **Day 28: End of the assay.**
 - a. ATP quantification assay of one 96-well ULA plate.

Appendix E

Bile acids mix preparation

Table 2 – Bile acids mix preparation.

Bile acids	[2 000x concentrated bile acids] (mM)	Molecular weight (g/mol)	Calculated mass (mg)	DMSO (mL)	Williams' Medium E (mL)
Glycochenodeoxycholic acid (GCDCA)	79.2	471.61	37.35	-	1
Chenodeoxycholic acid (CDCA)	23.4	392.57	9.19	1	-
Glycodeoxycholic acid (GDCA)	22.8	471.6	10.75	-	1
Deoxycholic acid (DCA)	24	414.55	9.95	1	-
Glycocholic acid (GCA)	21	465.62	9.78	1	-

Appendix F

Cholestatic Index assay plates layout

96-well deep well plate layout:

[Cyclosporine A] (μM)
 [Cyclosporine A] + Bile acids (μM)

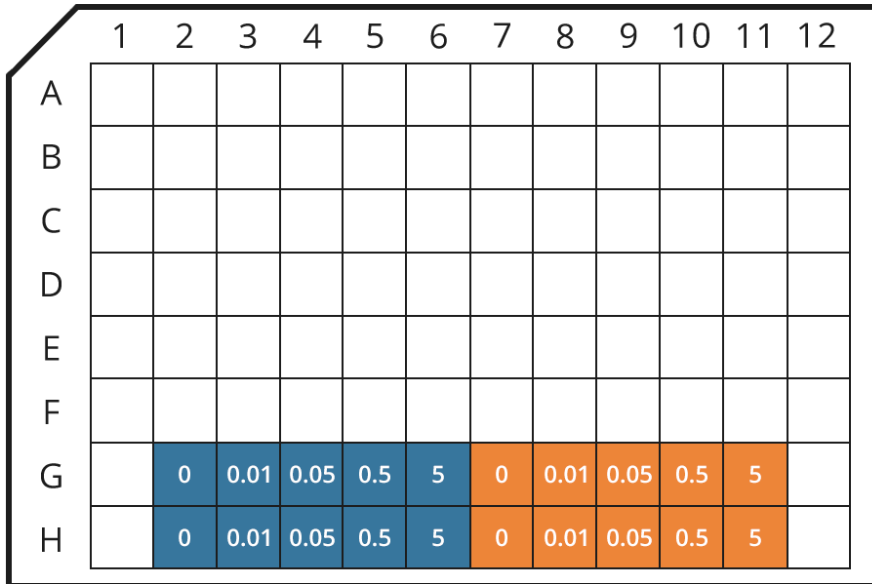


Figure 13 – 96-well deep well plate layout of cyclosporine A dilutions with and without bile acids.

96-well ultra-low attachment plate layout:

[Cyclosporine A] (μM)
 [Cyclosporine A] + Bile acids (μM)

 Phosphate-buffered saline (PBS)

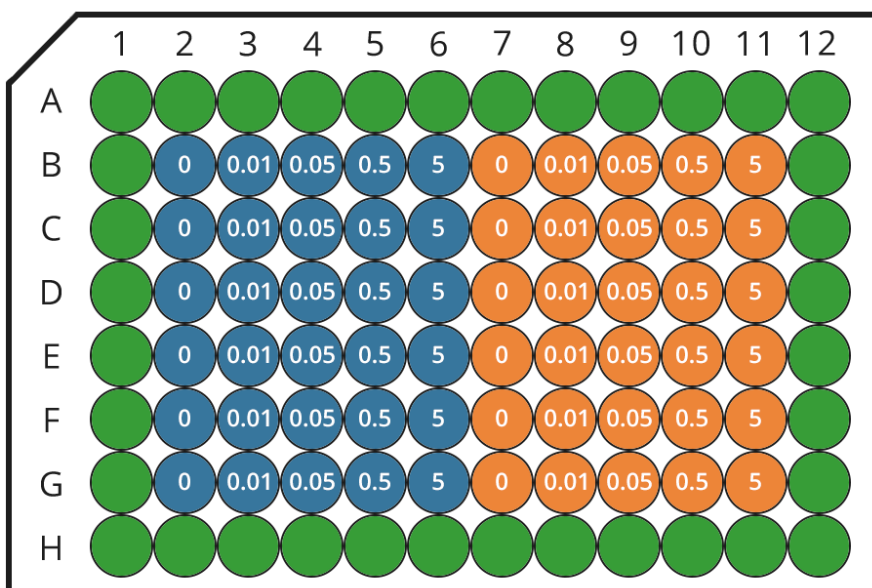


Figure 14 – 96-well ultra-low attachment plate layout of cyclosporine A exposure with and without bile acids.

Appendix G

Hanks' balanced salt solution (HBSS) composition (52)

Inorganic salts:

- Calcium chloride (CaCl_2) (anhydrous) – 1.26 mM
- Magnesium chloride ($\text{MgCl}_2 \cdot 6 \text{H}_2\text{O}$) – 0.49 mM
- Magnesium sulfate ($\text{MgSO}_4 \cdot 7 \text{H}_2\text{O}$) – 0.41 mM
- Potassium chloride (KCl) – 5.33 mM
- Potassium phosphate monobasic (KH_2PO_4) – 0.44 mM
- Sodium bicarbonate (NaHCO_3) – 4.17 mM
- Sodium chloride (NaCl) – 137.93 mM
- Sodium phosphate dibasic (Na_2HPO_4) (anhydrous) – 0.34 mM

Other components:

- D-glucose (dextrose) – 5.56 mM